

Articles

Mechanism of the $B(C_6F_5)_3$ -Catalyzed Reaction of Silyl Hydrides with Alkoxysilanes. Kinetic and Spectroscopic Studies

Julian Chojnowski,^{*,†} Sławomir Rubinsztajn,[‡] James A. Cella,[‡]
Witold Fortuniak,[†] Marek Cypryk,[†] Jan Kurjata,[†] and Krzysztof Kaźmierski[†]

Center of Molecular and Macromolecular Studies, Polish Academy of Sciences,
Sienkiewicza 112, 90-363 Łódź, Poland, and General Electric Company,
Global Research Center, Niskayuna, New York 12309

Received July 6, 2005

The coupling reaction of silyl hydrides with alkoxysilanes to produce siloxanes and hydrocarbons catalyzed by tris(pentafluorophenyl)borane was studied by gas chromatography and UV spectroscopy using model reagent systems: $Ph_2MeSiH + Ph_2MeSiOn-Oct$ (I) and $Ph_2MeSiH + Me_3SiOn-Oct$ (II). Detailed kinetic studies performed for system I showed that the reaction is first order in both substrates and the rate is proportional to the catalyst concentration. A highly negative apparent entropy of activation points to a crowded transition state structure, leading to a significant dependence of the rate on steric effects. Studies of system II demonstrated that the exchange of the Si–H and Si–OR functionality accompanies the coupling process and in many cases is the dominating reaction in this system. Ultraviolet spectra recorded during the reaction show a distinct strong absorption band with $\lambda_{max} = 303–306$ nm, which is due to an allowed electronic transition in the uncomplexed $B(C_6F_5)_3$ molecule. This absorption also gives rise to intense fluorescence with a maximum of the emission band at 460 nm. When the borane is complexed by oxygen nucleophiles, such as water, alcohol, or silanol and is not active as a catalyst, it does not show the absorption in the 303–306 nm region. This absorption may serve as a measure of the concentration of the active uncomplexed catalyst in the reaction system. Since complexes of $B(C_6F_5)_3$ with the alkoxysilane substrates and the disiloxane products are relatively weak, the catalyst appears in the reaction system mostly as an uncomplexed species and its concentration is not significantly changed during the reaction. The mechanism proposed includes the transient formation of a complex between hydrosilane, borane, and alkoxysilane in which H^- is transferred from silicon to boron and an oxonium ion moiety is generated by interaction of alkoxysilane with positive silicon. The decomposition of the complex occurs by the H^- transfer to one of the three electrophilic centers of the oxonium structure, which explains the competition between the siloxane formation and the Si–H/Si–OR exchange. In the case of alkoxysilanes derived from primary alcohols, H^- is preferably transferred to silicon. However, for alkoxysilanes derived from a secondary alcohol, such as isopropyl alcohol, the secondary carbon is more readily attacked than silicon by H^- , which leads to a high yield of mixed disiloxane.

Introduction

Tris(pentafluorophenyl)borane is a powerful and selective catalyst for many reactions in organic chemistry (for reviews see refs 1–3). This compound is particularly

active in promoting the reduction of an organic functionality with silyl hydrides. Parks and Piers⁴ found that $B(C_6F_5)_3$ catalyzes the hydrosilylation of carbonyl compounds. Since then, many other reductive processes using the $R_3SiH/B(C_6F_5)_3$ system have been reported. This system is particularly useful in the transformation of aldehydes, ketones, carboxylic acids, and their derivatives into silyl ethers,^{4,5} but further reduction to hydrocarbons also occurs smoothly.^{6–8} Hydrosilylation

* To whom correspondence should be sent. E-mail: jchojnow@bilbo.cbmm.lodz.pl.

[†] Polish Academy of Sciences.

[‡] General Electric Company.

(1) (a) Piers, W. E.; Chivers, T. *Chem. Soc. Rev.* **1997**, *26*, 345. (b) Piers, W. E. *Adv. Organomet. Chem.* **2005**, *52*, 1.

(2) Ishihara, K.; Yamamoto, H. *Eur. J. Org. Chem.* **1999**, 527, 7.

(3) Coates, G. W.; Hustal, P. D.; Reinartz, S. *Angew. Chem., Int. Ed.* **2003**, *41*, 2236.

(4) Parks, D. J.; Piers, W. E. *J. Am. Chem. Soc.* **1996**, *118*, 9440.

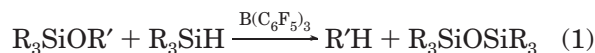
(5) Parks, D. J.; Blackwell, J. M.; Piers, W. E. *J. Org. Chem.* **2000**, *65*, 3090.

Table 1. Results of Preliminary Studies of the Condensation of Triorganohydrosilanes with Triorganoalkoxysilanes

	substrate ^a		[B(C ₆ F ₅) ₃] ₀ (10 ⁻³ mol/L)	approx <i>t</i> _{1/2} of R ₃ SiH conversion	time of quenching of reaction	[R ₃ SiOSiR ₃]/ [R' ₃ SiOSiR' ₃] (mol/mol)	substrate conversion		main byproduct ^b (mol %)
	R ₃ SiH	R' ₃ SiOR''					R ₃ SiH	R' ₃ SiOR''	
1	Et ₃ SiH	Me ₃ SiOMe	2.5			1.6	100	100	Et ₃ SiOMe (18)
2	Et ₃ SiH	Me ₃ SiOEt	2.5	~400 s	3 h	1.0	100	100	Et ₃ SiOEt (36)
3	Et ₃ SiH	Me ₃ SiOn-Oct	1.5	~1000 s	3 h	1.0	83	88	Et ₃ SiOn-Oct (6)
4	PhMe ₂ SiH	Me ₃ SiOMe	4.0	<20 s	10 min	1.5	100	100	PhMe ₂ SiOMe (5)
5	PhMe ₂ SiH	Me ₃ SiOEt	4.0	<20 s	20 min	1.5	100	100	PhMe ₂ SiOEt (2)
6	PhMe ₂ SiH	Me ₃ SiOn-Oct	3.0	<20 s	20 min	1.1	100	100	PhMe ₂ SiOn-Oct (<2)
7	Ph ₂ MeSiH	Me ₃ SiOn-Oct	0.6	30 s	0.5 h	1.2	83	100	Ph ₂ MeSiOn-Oct (10)
8	Ph ₂ MeSiH	Me ₃ SiOi-Pr	11.6	1000 s	3.5 h	0.01	97	98	Ph ₂ MeSiOCMe ₂ SiMe ₃ Me ₃ SiOCMe ₂ SiPh ₂ Me (5)
9	Ph ₂ MeSiH	Et ₃ SiOi-Pr	2.0	~120 h	23 h	<0.01	12	11	

^a Initial molar ratio of substrates was 1:1, neat, room temperature. ^b Me₃SiOSiMe₃ and Me₃SiH were not controlled.

of enones involving 1,4-addition of hydrosilanes proceeds selectively, affording silyl enol ethers.⁹ The reduction of imines to tertiary amines via a silylammonium intermediate^{10,11} and the selective hydrosilylation of some olefins¹² are also catalyzed by B(C₆F₅)₃. As an example of the latter, the pure β -addition of hydrosilanes to styrene without a side polymerization process has been reported. The silylation of alcohols with the formation of H₂ as the only byproduct¹³ and the cleavage of silyl ether and ether bonds catalyzed by B(C₆F₅)₃^{6,14} provide an easy and convenient route for the reduction of primary, secondary, and tertiary alcohols as well as some ethers to corresponding hydrocarbons. The intermediate product in the reduction of the oxygen function by R₃SiH/B(C₆F₅)₃ is a silylalkyl ether (alkoxysilane), which further reacts with another equivalent of hydrosilane to form a hydrocarbon according to eq 1.¹⁴

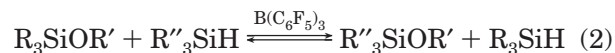


Reaction 1 often occurs rapidly and quantitatively under mild conditions, making it a useful method in organosilicon chemistry for the generation of siloxane bonds.^{15–17} This method of forming siloxanes could be very attractive since the starting materials for this process are often inexpensive and easy to handle. The byproduct of this condensation is a neutral and harmless aliphatic hydrocarbon. The purpose of this work is to study reaction 1 using model reactants to shed more light on the mechanism of this process. We believe that the deeper understanding of this process not only will permit its broader use in the organosilicon chemistry

but will also provide additional information on a reaction that is of considerable importance in organic synthesis.

Results and Discussion

Kinetic Studies. Synthetic organic chemists for whom the siloxane is only a byproduct of the reaction have made use of reaction 1. Our primary concern was to gather information about the course of the reaction primarily as a process for formation of siloxane bonds. Our first observation was that eq 1 is followed only in the case when substituents R at silicon were the same in both reactants, alkoxysilane and hydrosilane. When silanes with different R₃Si moieties were used, the exchange process, depicted in eq 2, was observed as a process accompanying siloxane formation.



Reaction 2 generates a new alkoxysilane and hydrosilane pair of substrates for the redox condensation according to eq 1. Since cross-reactions between the initial and secondary pairs of reactants may occur, three disiloxanes are produced: the expected unsymmetrical disiloxane, R₃SiOSiR''₃, and two symmetrical disiloxanes, R₃SiOSiR₃ and R''₃SiOSiR''₃. Several reactions of various trimethylalkoxysilanes with triorganohydrosilanes were carried out and followed by gas chromatography. Approximate ratios of the symmetrical higher molecular weight disiloxane to the unsymmetrical one in some coupling reactions are given in Table 1.

In most cases studied the symmetrical disiloxanes are the main SiOSi products, so much that the statistical factor of 2 should be taken into account. However, the unsymmetrical disiloxane is almost the exclusive product when an isopropoxysilane is used as substrate. In this case the exchange process (reaction 2) is of much less importance. The formation of the Et₃SiH intermediate was not observed in the reaction of Ph₂MeSiH + Et₃SiOi-Pr. Ph₂MeSiOi-Pr was not formed either; however, small amounts (about 5%) of two isomeric products of H₂ abstraction with 1,2-silyl migration were detected in the products of reaction of Ph₂MeSiH + Me₃SiOi-Pr (Table 1, entry 8, last column).

The coupling of Et₃SiH with Me₃SiOR occurs more slowly than the respective reactions of PhMe₂SiH and Ph₂MeSiH. Considerable amount of Et₃SiOR intermediates remain unreacted in the Et₃SiH + Me₃SiOR reac-

(6) Gevorgyan, V.; Rubin, M.; Benson, S.; Liu, J.-X.; Yamamoto, Y. *J. Org. Chem.* **2000**, *65*, 6179.

(7) Gevorgyan, V.; Rubin, M.; Liu, J.-X.; Yamamoto, Y. *J. Org. Chem.* **2001**, *66*, 1672.

(8) Bajracharya, G. B.; Nogami, T.; Jin, T.; Matsuda, K.; Gevorgyan, V.; Yamamoto, Y. *Synth.-Stuttg.* **2004**, 308.

(9) Blackwell, J. M.; Morrison, D. J.; Piers, W. E. *Tetrahedron* **2002**, *58*, 8247.

(10) Blackwell, J. M.; Sonmor, E. R.; Scoccitti, T.; Piers, W. E. *Org. Lett.* **2000**, *2*, 3921.

(11) Blackwell, J. M.; Piers, W. E.; Parvez, M. *Org. Lett.* **2000**, *2*, 695.

(12) Rubin, M.; Schwiier, T.; Gevorgyan, V. *J. Org. Chem.* **2002**, *67*, 1936.

(13) Blackwell, J. M.; Foster, K. L.; Beck, V. H.; Piers, W. E. *J. Org. Chem.* **1999**, *64*, 4887.

(14) Gevorgyan, V.; Liu, J.-X.; Rubin, M.; Benson, S.; Yamamoto, Y. *Tetrahedron Lett.* **1999**, *40*, 8919.

(15) Rubinsztajn, S.; Cella, J. (GE Company) US Pat. Application 200/0127668 A1, 2002.

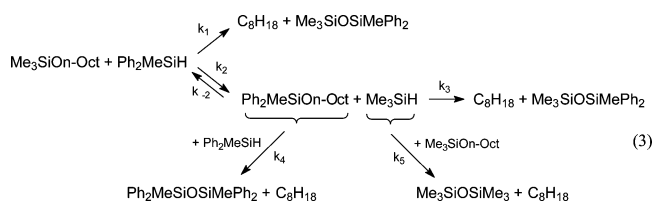
(16) Rubinsztajn, S.; Cella, J. *Polym. Prepr.* **2004**, *45*, 635.

(17) Rubinsztajn, S.; Cella, J. *Macromolecules* **2005**, *38*, 1061.

tion systems, which means that Et_3SiOR is also less reactive than corresponding PhMe_2SiOR and $\text{Ph}_2\text{-MeSiOR}$. A steric effect in the alkoxy group is important, as isopropoxy silane reacts much less readily than the ethoxy and *n*-octyloxy homologues.

The system $\text{Ph}_2\text{MeSiH} + \text{Me}_3\text{SiOn-Oct}$ was chosen for more detailed kinetic investigations for two reasons. First, the moderate rate of the reaction makes it possible to easily follow the overall process, and second, the substrates and products are not volatile and are thus readily sampled for concentration monitoring. Gas chromatographic analysis permitted the determination of six of the eight species present in the reaction system. The course of the reaction is presented in Figure 1.

Results correspond to the reaction scheme represented by eqs 3. It has also been determined in a



separate experiment that a cleavage of the siloxane bond in the reaction of PhMe_2SiH with hexamethyldisiloxane does not occur under the same reaction conditions. Thus, we can consider the condensation reactions leading to the formation of siloxane bond as irreversible.

A computer simulation method permitted us to determine approximate values of the catalytic constants of the component reactions in the system. These rate constants in $\text{kg}^2/\text{mol}^2 \text{ s}$ are $k_1 = 3$, $k_2 = 20$, $k_{-2} = 25$, $k_3 = 3$, $k_4 = 2$, and $k_5 = 20$. Thus, the exchange of hydride and alkoxy groups is faster than the condensation of substrates to form siloxanes in the system studied.

The coupling represented by eq 4, which constitutes the component reaction of process 3, was the subject of more comprehensive kinetic studies, which led to the more precise determination of the specific rate constant k_4 .



The purpose was to determine kinetic law, rate constants, and apparent activation parameters of this reaction, which is considered to be a simple model of the $\equiv\text{SiH} + \text{ROSi}\equiv$ coupling. A series of kinetic runs were carried out at various concentrations and temperatures. A typical example of a kinetic run is shown in Figure 2. Both reactants enter the reaction at the same rate, and both products of the reaction are formed at the same rate.

It is shown in Figure 3 that the reaction proceeds according to the second-order kinetic law to more than 85% conversion of reactants. The reaction is first order in hydrosilane and first order in alkoxyasilane. This is demonstrated in Figure 4, where the conversion starting with unequal initial concentrations of reactants is presented in the second-order plot; that is, the absolute value of $\log([\text{Ph}_2\text{MeSiH}]/[\text{Ph}_2\text{MeSiOn-Oct}])$ is plotted against time. The specific rate of the coupling process (Table 2) is proportional to the catalyst concentration;

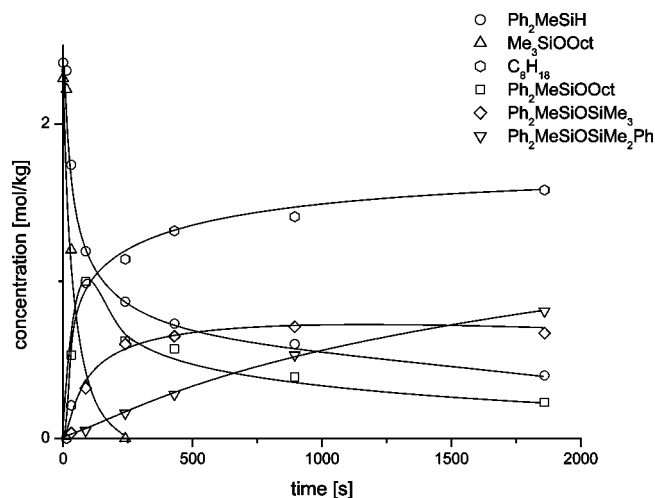


Figure 1. Substrate conversion, product formation, and intermediate concentration vs time dependence for the reaction $\text{Ph}_2\text{MeSiH} + \text{Me}_3\text{SiOn-C}_8\text{H}_{17}$; $[\text{B}(\text{C}_6\text{F}_5)_3] = 6.44 \times 10^{-4} \text{ mol}\cdot\text{kg}^{-1}$, neat, 25°C .

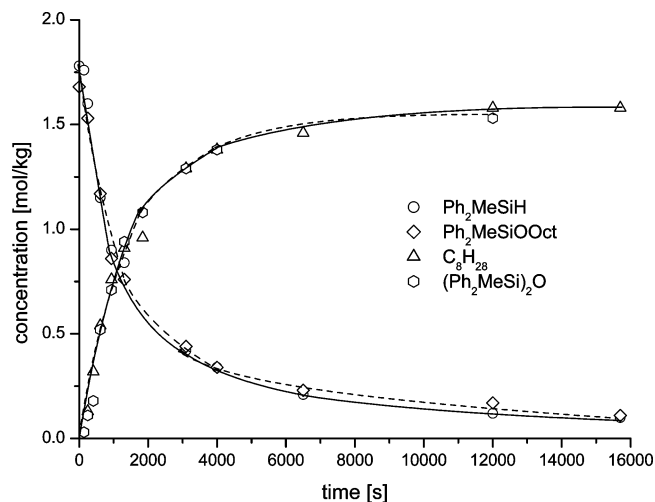


Figure 2. Substrate conversion and product formation vs time dependence for the reaction $\text{Ph}_2\text{MeSiH} + \text{Ph}_2\text{MeSiOn-C}_8\text{H}_{17}$ catalyzed by $(\text{C}_6\text{F}_5)_3\text{B}$; $[\text{B}(\text{C}_6\text{F}_5)_3] = 2.08 \times 10^{-4} \text{ mol}\cdot\text{kg}^{-1}$, neat, 25°C .

thus, the reaction follows closely the kinetic law represented by eq 5.

$$-\frac{d[\equiv\text{SiH}]}{dt} = -\frac{d[\equiv\text{SiOR}]}{dt} = \frac{d[\equiv\text{SiOSi}\equiv]}{dt} = \frac{d[\text{RH}]}{dt} = k[\text{B}(\text{C}_6\text{F}_5)_3][\equiv\text{SiH}][\equiv\text{SiOR}] \quad (5)$$

From kinetic experiments performed at different temperatures the following apparent activation parameters were deduced: $E_A = 7.3 \text{ kcal/mol}$, $\Delta H^\ddagger = 6.7 \text{ kcal/mol}$, $\Delta S^\ddagger = -33.8 \text{ eu}$. The reaction exhibits a very low energy barrier and high negative activation entropy. The latter reflects high steric requirements in the formation of the transition state.

Theoretical and Spectroscopic Studies of the Interaction in the $\equiv\text{SiOR} + \equiv\text{SiH} + \text{B}(\text{C}_6\text{F}_5)_3$ System. Earlier studies of the interaction of triorganohydrosilanes with $\text{B}(\text{C}_6\text{F}_5)_3$ using ^1H , ^{29}Si , and ^{19}F NMR⁵ showed that this interaction does not cause a significant perturbation of the NMR spectra of the borane or of the silane expected for the formation of a

Table 2. Kinetic Results of the Condensation of Ph₂MeSiH with Ph₂MeSiOn-Oct at Equal Initial Concentration of Substrates, Neat

no.	B(C ₆ F ₅) ₃ , 10 ⁴ mol·kg ⁻¹	[Ph ₂ MeSiH] ₀ , mol·kg ⁻¹	second-order specific rate <i>k</i> ₄ , 10 ³ kg mol ⁻¹ s ⁻¹	conversion range, %	<i>r</i>	catalytic constant <i>k</i> _{cat} , kg ² mol ⁻¹ s ⁻¹	temp, °C
1	2.08	1.74 (8)	0.645	81	0.996	3.10	25.5
2	4.84	1.84	1.47	91	0.997	3.04	25
3	9.36	1.95	2.83	72	0.998	3.02	25
4	2.12	1.66	1.09	90	0.998	5.14	40.0
5	2.33	1.67	2.53	87	0.997	10.9	59.4

strong complex. This was confirmed by our observations. When an excess of Et₃SiH was introduced to a methylene chloride solution of B(C₆F₅)₃, only a small upfield shift of the para-F signal was observed and a δ(p-F) – δ(m-F) difference as large as 17.2 ppm was observed. Generally, a strong interaction of the borane with electron-donating species gives rise to a small δ(p-F) –

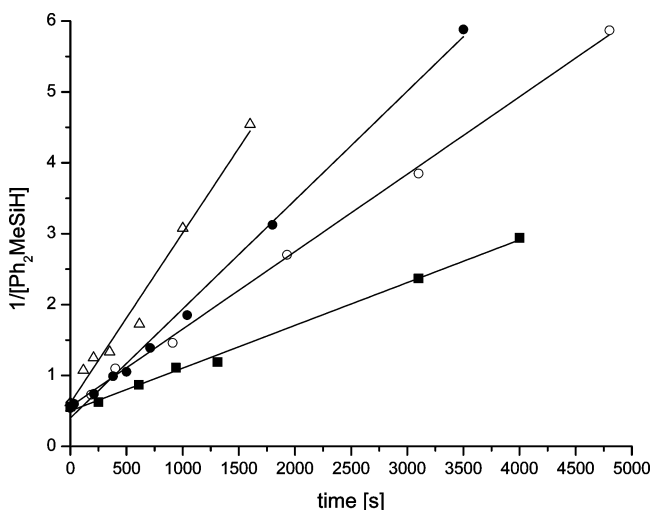


Figure 3. Second-order plot for the coupling reaction of Ph₂MeSiH with Ph₂MeSiOn-C₈H₁₇ for runs at equal initial concentrations of substrates. Concentrations of B(C₆F₅)₃ in mol·kg⁻¹ and temperatures were (■) 2.08 × 10⁻⁴, 25 °C; (○) 2.12 × 10⁻⁴, 40 °C; (●) 4.84 × 10⁻⁴, 25 °C; (△) 2.33 × 10⁻⁴, 59.4 °C. [SiH]₀ = [SiOn-Oct]₀ in most cases was 1.68 mol·kg⁻¹.

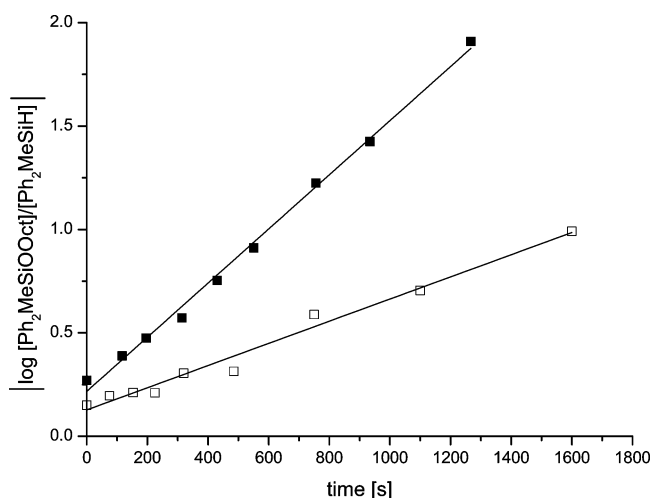


Figure 4. Second-order plot for the coupling reaction of Ph₂MeSiH with Ph₂MeSiOnC₈H₁₇ for runs at unequal initial concentrations of substrates, 25 °C. Concentrations in kg·mol⁻¹ were (□) [B(C₆F₅)₃] = 9.4 × 10⁻⁴, [≡SiH]₀ = 1.90, [≡SiOn-Oct]₀ = 1.38; (■) [B(C₆F₅)₃] = 1.4 × 10⁻³, [≡SiH]₀ = 1.1, [≡SiOn-Oct]₀ = 2.1. The absolute values of log[Ph₂MeSiOn-Oct]/[Ph₂MeSiH] are plotted against time.

δ(m-F) difference.¹⁸ The spectrum did not change much after the introduction of an excess of Ph₂MeSiOn-Oct.

Theoretical calculation by the semiempirical AM1 method for R₃SiH···B(C₆F₅)₃ (R = Et or Ph) performed by Parks et al.⁵ pointed to a rather significant change of Mulliken charges on the borane and silane moieties. Our calculations performed using more advanced quantum-mechanical DFT methods show that the silane–borane interaction in the Me₃SiH–B(C₆F₅)₃ model complex is very weak (Δ*E* = –3.4 kcal/mol at B3LYP/6-31G* and Δ*E* ≈ 0 at the B3LYP/6-311+G(2d,p)//B3LYP/6-31G* level). The Si–H–B arrangement is nonlinear (∠SiHB = 155.7°) with a rather long H–B distance of 2.842 Å, and the distortion of the BC₃ skeleton from planarity is negligible. Charge transfer from silane to borane, as measured by comparison of natural population atomic (NPA) charges in reagents and in the complex, is essentially zero. The Wiberg bond order for H–B is 0.011 and that for Si–B is 0.005. The change in Si–H bond order upon complexation is insignificant, from 0.906 in free silane to 0.881 in the complex with borane. These features confirm that the interaction is indeed very weak.

The general conclusion of this part of the spectral and theoretical studies was that both complexes, ≡SiH + B(C₆F₅)₃ and possibly also ≡SiOR + ≡SiH + B(C₆F₅)₃, are relatively weak and the equilibrium of their formation in the reaction system lies strongly to the side of uncomplexed species.

A UV spectroscopic study was also performed. Triarylboranes are known to exhibit a broad long-wavelength absorption in the ultraviolet region between 250 and 370 nm.¹⁹ Triphenyl borane in methylene chloride shows in this range two intensive bands with maxima at 287.1 and 275.7 nm, with molar extinction values at a maximum of ε_{max} = 39 000 and 35 000, respectively. This absorption is interpreted by intramolecular charge transfer (CT) from π benzene ring orbitals to the empty p orbital of boron. Their origin is analogous to the origin of the absorption in the visible region of corresponding triarylcarbenium ions, which are isoelectronic species with boranes.

We examined the spectra of (C₆F₅)₃B solution in methylene chloride and in toluene. To our knowledge, the electronic spectroscopy of this borane has not been studied yet. The long-wavelength absorption of this compound is observed as a band with λ_{max} = 303 nm, ε_{max} = 2.0 × 10⁴ (CH₂Cl₂). In toluene the band is slightly shifted to longer wavelength, λ_{max} = 306 nm. The spectrum of the borane in methylene chloride solution is presented in Figure 5.

(18) Köhler, K.; Piers, W. E.; Xin, S.; Feng, Y.; Bravakis, A. M.; Jarvis, A. P.; Clegg, W.; Yap, G. P. A.; Marder, T. B. *Organometallics* **1998**, *17*, 3557.

(19) Ramsay, B. G. *J. Phys. Chem.* **1966**, *70*, 611.

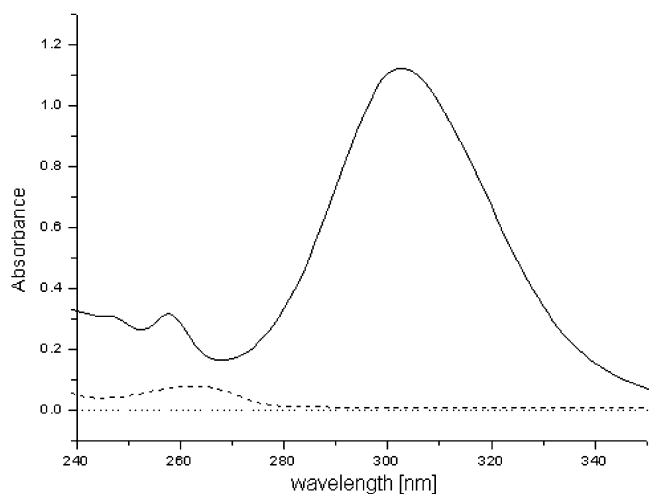


Figure 5. UV spectra of the solution of $B(C_6F_5)_3$ in methylene chloride (solid line) and the spectra of $B(C_6F_5)_3$ complexed with water (dashed line). $[B(C_6F_5)_3] = 0.5 \times 10^{-4} \text{ mol} \cdot \text{dm}^{-3}$. A small amount of Et_3SiH was introduced before taking the spectrum of $B(C_6F_5)_3$ to remove traces of water.

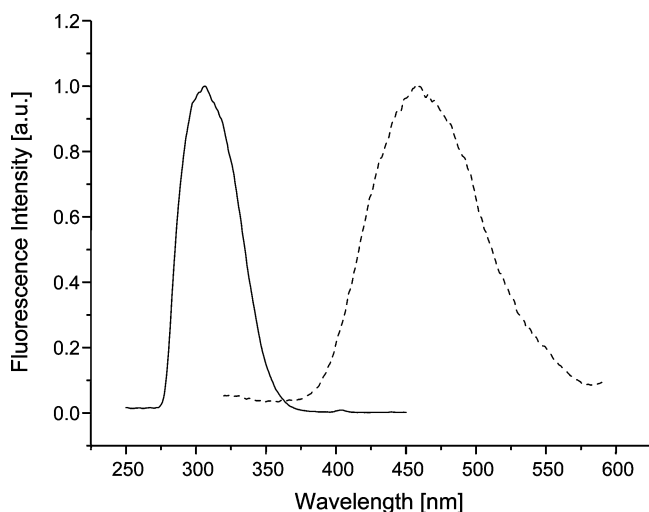


Figure 6. Fluorescence spectrum of $B(C_6F_5)_3$, λ (excitation) = 303 nm (solid line) and the excitation spectra (dashed line), λ (emission) = 460 nm of the solution of $[Et_3SiH]_0 = 6 \times 10^{-2} \text{ mol} \cdot \text{dm}^{-3}$ and $[B(C_6F_5)_3]_0 = 1 \times 10^{-5}$ in methylene chloride. Et_3SiH was introduced to remove traces of water.

This long-wavelength absorption of $B(C_6F_5)_3$ leads to fluorescence. An intense emission band is observed when the solution of the borane is irradiated with light at $\lambda = 303 \text{ nm}$ (Figure 6). The maximum of the emission occurs at 460 nm; thus the fluorescence band overlaps the visible range.

The UV spectrum of $B(C_6F_5)_3$ was also calculated using a time-dependent DFT model (TD-B3LYP/6-31+G*); see Table 3. The six lowest transitions were calculated, showing only one very strong band at 329 nm consisting of two degenerate $\pi \rightarrow \text{LUMO}$ excitations involving transition of π electrons of the rings to the LUMO orbital, which consists mainly of the empty p_B orbital together with a small admixture of π^* orbitals from the rings. We have also calculated the spectrum (six lowest excitations) of the $Me_3SiH-B(C_6F_5)_3$ complex. Since the geometry of the borane fragment in the complex is very close to that of the borane alone, the spectrum is not very different. Two strong absorptions

Table 3. Calculated (TD-DFT) UV Spectra (only for singlet excited states) of $B(C_6F_5)_3$ and Its Complexes with H_2O and Me_3SiH

	wavelength (oscillator strength)
$B(C_6F_5)_3$	365.6 (0.01), 354.6 (2×0.0001), 329.5 (2×0.26), 281.6 (≈ 0)
$Me_3SiH-B(C_6F_5)_3$	358 (0.01), 325.8 (0.23), 324.2 (0.24), 289.9 (0.03)
$H_2O-B(C_6F_5)_3$	254.6 (0.01), 246.5 (0.009), 243.4 (0.014), 237.6 (0.013), 236.9 (0.02)

at 324 and 326 nm are observed, corresponding to the analogous $\pi \rightarrow \text{LUMO}$ transitions in borane. The LUMO in the complex is almost identical to the LUMO in borane itself.

The absorbance of $B(C_6F_5)_3$ due to the internal charge transfer (bands at 303 nm) disappears completely when the borane is engaged in a complex with water, alcohol, or silanol. The reason is that the p orbital of boron is occupied by electrons of the donor and is not available for the electrons of the benzene ring. Second, the geometry of the borane is changed upon complexation toward tetrahedral, which disfavors the overlap between donor and acceptor orbitals. This is well documented by calculations for the $H_2O-B(C_6F_5)_3$ complex, which show that UV absorption above 260 nm disappears completely. These calculations predict only several weak absorption bands in the range 235–255 nm (Table 3). However, a weak absorption band in the spectrum of the complex in CH_2Cl_2 with maximum at 264 nm is observed (Figure 5). Complexes of $B(C_6F_5)_3$ with water and alcohols have already been the subject of extensive research.^{20–22}

In contrast to a strong interaction of $B(C_6F_5)_3$ with water and other hydroxyl donors, the borane interaction with silicon ether type donors, disiloxanes and alkoxy-silanes, is very weak. Addition of disiloxane has almost no effect on absorption in the $B(C_6F_5)_3 + Et_3SiH$ system, and the addition of an alkoxy-silane has little effect on this absorption. In contrast, the addition of a small amount of water, not much larger than stoichiometric, eliminates the absorption, which, however, is regained as soon as water is immediately removed by the borane–hydrosilane system.

Similarly, if excess methanol is added to $B(C_6F_5)_3 + R_3SiH$ at the amount smaller than that of R_3SiH , the band due to the internal CT complex disappears, but after some time appears again. This behavior is a result of the conversion of alcohol with the participation of a small amount of the $\equiv SiH-B(C_6F_5)_3$ complex remaining in equilibrium with the alcohol– $B(C_6F_5)_3$ complex. Although the concentration of this complex is initially extremely small, it increases as methanol is converted to methane. However, if a considerable amount of water or alcohol is present in the system, it may permanently suppress the $\equiv SiH-B(C_6F_5)_3$ complex formation. The much stronger interaction of water than ethers not only is the result of its higher basicity and lower steric requirements but also is due to hydrogen bonds formed by the complexed water molecule with ortho fluorine

(20) Jacobsen, H.; Berke, H.; Döring, S.; Kehr, S.; Erker, G.; Fröhlich, R.; Meyer, O. *Organometallics* **1999**, *18*, 1724.

(21) Bergquist, C.; Bridgewater, B. M.; Harlan, C. J.; Norton, J. R.; Fiesner, R. A.; Parkin, S. *J. Am. Chem. Soc.* **2000**, *122*, 10581.

(22) Beringhelli, T.; Maggiani, D.; Alfonso, G. A. *Organometallics* **2001**, *20*, 4927.

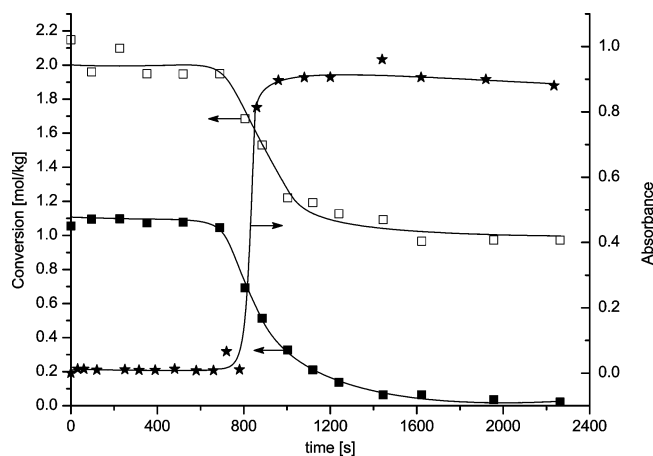


Figure 7. Conversion–time plots for the reaction $\text{Ph}_2\text{MeSiH} + \text{Ph}_2\text{MeSiOn-Oct}$ catalyzed by $\text{B}(\text{C}_6\text{F}_5)_3$ monitored by gas chromatography and the UV absorbance–time plot monitored at $\lambda = 335$ nm, path length 0.1 cm. $[\text{B}(\text{C}_6\text{F}_5)_3] = 1.4 \times 10^{-3} \text{ mol}\cdot\text{kg}^{-1}$, 25°C . (\square) $\text{Ph}_2\text{MeSiOn-Oct}$, (\blacksquare) Ph_2MeSiH , (\star) UV absorbance.

atoms of the benzene rings. This interaction is clearly indicated in the B3LYP/6-31G*-optimized structure of the water– $\text{B}(\text{C}_6\text{F}_5)_3$ complex (see Supporting Information). The B3LYP/G-311+G(2d,p)//B3LYP/6-31G* energy of complex formation of $\text{H}_2\text{O} - \text{B}(\text{C}_6\text{F}_5)_3$ is -8.4 kcal/mol.

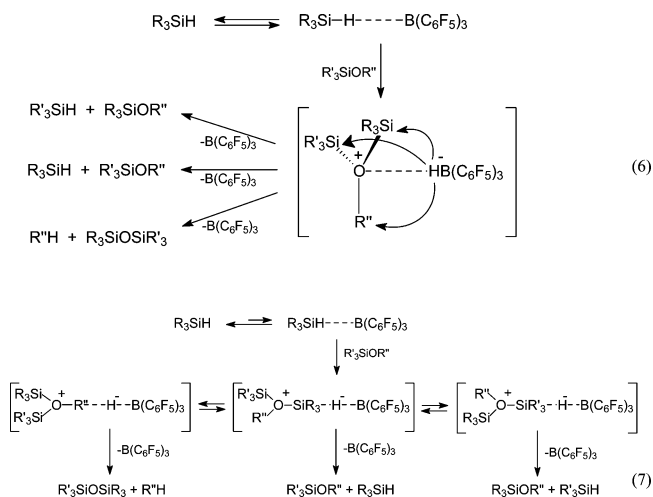
Since the concentration of the $\text{R}_3\text{SiH} - \text{B}(\text{C}_6\text{F}_5)_3$ complex in the reaction system is very low, it may be assumed that the absorption by the reaction system in the region of the internal CT band of $(\text{C}_6\text{F}_5)_3\text{B}$ is solely due to uncomplexed borane. Therefore, the absorption may be used to monitor the free borane in the reaction system.

Simultaneous examination of the UV spectra and the course of the reaction by gas chromatography was carried out for the reaction system of $\text{Ph}_2\text{MeSiOn-Oct} + \text{Ph}_2\text{MeSiH}/\text{B}(\text{C}_6\text{F}_5)_3$. Unpurified substrates, which had not been dried before, were used in this experiment to allow for a significant induction period in the reaction during which the $\equiv\text{SiH} - \text{B}(\text{C}_6\text{F}_5)_3$ complex reaches a critical level for catalytic activity. In this period the borane forms the complex with a hydroxylic contaminant, mostly water (water content in the sample, as estimated from the amount of initially formed disiloxane, was about $2 \times 10^{-2} \text{ mol}\cdot\text{kg}^{-1}$, at least 1 order more than that of the catalyst), and is not able to form a sufficient amount of the $\equiv\text{SiH} - \text{B}(\text{C}_6\text{F}_5)_3$ complex to catalyze the coupling reaction but is sufficient to catalyze much faster conversion of the undesired contaminant. The conversion of substrates and the variation of the absorbance at 335 nm are presented in Figure 7, which demonstrate the inhibition of the reaction by water. There is a clear correlation of the free $\text{B}(\text{C}_6\text{F}_5)_3$ formation monitored by UV and the course of the reaction. The reaction starts exactly at the moment when the band of uncomplexed $\text{B}(\text{C}_6\text{F}_5)_3$ appears. The absorption maintains a constant level, although the concentration of Ph_2MeSiH drops down to almost zero, which excludes any contribution from the $\text{Ph}_2\text{MeSiH} - \text{B}(\text{C}_6\text{F}_5)_3$ complex to the absorption measured. Therefore the concentration of uncomplexed $\text{B}(\text{C}_6\text{F}_5)_3$ is constant during the reaction. These data corroborate well with the regular second-order course of the reaction observed

to a high conversion. They also give evidence that the intermediate complex must appear in a very small concentration (and confirm that the competitive formation of the borane–alkoxysilane and the borane–disiloxane has no effect on the reaction rate).

Mechanism of the $\equiv\text{SiH} + \text{ROSi} \equiv$ Coupling Process. A mechanism for reduction of aliphatic alcohols and ethers by triorganohydrosilanes in the presence of $\text{B}(\text{C}_6\text{F}_5)_3$ has been presented recently.⁶ The proposed mechanism involves activation of hydrosilane by reversible formation of a $\equiv\text{SiH} - \text{B}(\text{C}_6\text{F}_5)_3$ complex. The incipient silylium species coordinates the most basic function to yield an intermediate oxonium ion, which is subsequently reduced by hydride transfer from $[\text{HB}(\text{C}_6\text{F}_5)_3]^-$ to the alkyl group.

In general, our kinetic, spectral, and calculation results are in agreement with this mechanism. The question remains whether the full oxonium ion appears as an intermediate in this process. To check this possibility, we introduced into the reaction system considerable amounts of $\text{Ph}_3\text{C}^+\text{B}(\text{C}_6\text{F}_5)_4^-$, which in the presence of $\equiv\text{SiH}$ and $\equiv\text{SiOR}$ substrates should be rapidly converted to $\text{Ph}_3\text{CH} + (\equiv\text{Si})_2\text{OR}^+\text{B}(\text{C}_6\text{F}_5)_4^-$,^{23,24} leading to a considerable increase of the stationary oxonium ion concentration in the system. The addition of the trityl borate salt had no significant effect on the reaction rate. This result clearly showed that the oxonium ion is not formed as diffusively equilibrated species. The reactive intermediate is thus the complex in which hydride is transferred to the borane center interacting with one or more electrophilic centers of the oxonium moiety of the complex. A two- or three-center interaction structure of the complex (eq 6) corroborates well with the formation of products observed in this system. An alternative one-center interaction, eq 7, would assume a fast intramolecular rearrangement of the complex, leading to a change of the center interacting with the hydride ion.



In the decomposition of the intermediate complex the hydride ion is transferred to one of the three electrophilic centers of the oxonium moiety, leading to three directions of the reaction, one of which is re-formation

(23) Olah, G. A.; Li, X.-Y.; Wang, Q.; Rasul, G.; Prakash, G. K. S. *J. Am. Chem. Soc.* **1995**, *117*, 8962.

(24) Cypryk, M.; Kurjata, J.; Chojnowski, J. *J. Organomet. Chem.* **2003**, *686*, 373.

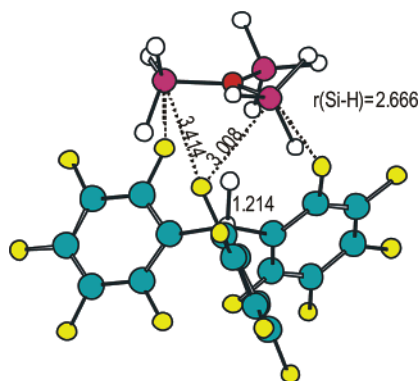
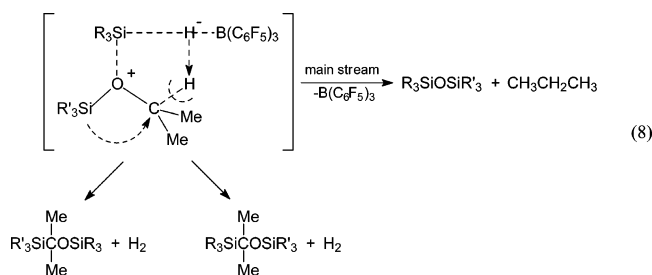


Figure 8. B3LYP/6-31G* geometry of the $(\text{H}_3\text{Si})_3\text{O}-\text{HB}(\text{C}_6\text{F}_5)_3$ complex. Si-F interactions are marked by dotted lines; interatomic distances are given in Å.

of substrates. Comparing silicon and primary carbon, the main factor seems to be the charge on the electrophilic centers. Silicon, because of its lower electronegativity, bears higher positive charge than carbon and more easily acquires negatively charged H^- . Instead, the secondary carbon, being a softer center than the primary carbon, can better compete for soft H^- with the harder silicon center, and in this case the formation of the hydrocarbon propane and disiloxane is the main direction of the process. However, the reduction of isopropoxysilane occurs more slowly than the analogous reaction with a primary alkoxysilane because of higher steric requirements for the formation of the intermediate complex including the isopropoxy-substituted oxonium ion.

In the case of the reaction of isopropoxysilane the decomposition of the intermediate complex strongly favors H^- transfer to carbon. Another possibility, however, is attack of H^- on hydrogen at the secondary carbon, resulting in the H_2 formation followed by 1,2-silyl group migration according to eq 8, while the attack on silicon plays only a marginal role.



To confirm the possibility of formation of the salt-like complex, we performed quantum-mechanical calculations for the simple $(\text{H}_3\text{Si})_3\text{O}-\text{HB}(\text{C}_6\text{F}_5)_3$ complex, which would result from the reaction of $\text{SiH}_4 + (\text{H}_3\text{Si})_2\text{O} + \text{B}(\text{C}_6\text{F}_5)_3$. Calculations showed that such highly symmetrical complex (C_3 symmetry) is the true minimum on the potential energy surface and therefore can be an intermediate in the reaction. The B3LYP/6-31G* geometry of this complex is presented in Figure 8.

Conclusions

The interaction of an alkoxytriorganosilane with a hydridotriorganosilane in the presence of $(\text{C}_6\text{F}_5)_3\text{B}$ leads to two processes: a redox that provides disiloxane and

hydrocarbon and a SiH and SiOR group exchange between substrates. In the case of a primary alkoxysilane the latter reaction is the favored path, producing the exchanged alkoxysilane and hydrosilane as kinetic products. The final products are those of the redox reactions leading to a hydrocarbon and three disiloxanes. If both reactants have the same triorganosilyl moiety, then the exchange process is invisible and the reaction produces the two expected products, hydrocarbon and hexaorganodisiloxane. The reaction is first order in the $\equiv\text{SiH}$ reagent and first order in alkoxysilane. The rate is proportional to the concentration of catalyst. The large negative entropy of activation is related to the considerable role of steric effects observed for the reaction. A relatively high rate of the reaction is the result of a low energy barrier, as suggested by theoretical calculations.

Studies of the UV spectral properties of the catalyst revealed that uncomplexed $\text{B}(\text{C}_6\text{F}_5)_3$ absorbs in the long-wavelength UV region $\lambda_{\text{max}} = 303$ nm (in methylene chloride). Irradiation at the λ_{max} of this band leads to intense blue fluorescence ($\lambda_{\text{em}} = 460$ nm).

Under conditions of the kinetic studies $\text{B}(\text{C}_6\text{F}_5)_3$ is present almost exclusively as the free species in the reaction system. A mechanism consistent with the kinetic and spectral data assumes the formation of an intermediate oxonium complex with a salt-like structure formed by both reactants and catalyst. The complex may decompose to regenerate starting substrates, exchange reaction products, or redox reaction products.

Strong preference for the redox reaction over the exchange process is observed when an alkoxysilane with a secondary carbon isopropoxy group was used as the substrate. However, steric effects make this reaction relatively slow.

Experimental Section

Chemicals. Tris(pentafluorophenyl)borane (Aldrich, reagent grade, newly purchased) was used without purification since the resublimation of $\text{B}(\text{C}_6\text{F}_5)_3$ under 10^{-3} Torr of argon, as proposed in ref 8, did not seem to improve its purity. For part of the spectral and some kinetic experiments $\text{B}(\text{C}_6\text{F}_5)_3$ was also synthesized by us using the Grignard reaction of BCl_3 with $\text{C}_6\text{F}_5\text{MgBr}$ according to ref 25. It was purified by formation of $\text{Et}_2\text{O} \cdot \text{B}(\text{C}_6\text{F}_5)_3$ complex as recommended in ref 25 and subsequent thermal decomposition of the complex and resublimation of $\text{B}(\text{C}_6\text{F}_5)_3$ under vacuum. The ^{19}F NMR analysis did not show any fluorine impurity.

Hydrosilanes. Ph_2MeSiH (ABCR GmbH) and PhMe_2SiH and Et_3SiH (both Gelest) were purified by distillation. Gas chromatographic (GC) analysis did not show any significant impurities.

Alkoxysilanes. Me_3SiOEt was purchased (Gelest), while Me_3SiOMe , $\text{Me}_3\text{SiOn-Oct}$, and $\text{Ph}_2\text{MeSiOn-Oct}$ were synthesized by the usual route, i.e., silylation of alcohol with chlorosilane/ Et_3N . They were refluxed with Na and distilled. Their purity was higher than 98%. *n*-Octane and *n*-dodecane (Sigma-Aldrich, purity > 98% as checked by GC) were used as received.

Solvents. Toluene (POCH, pure for analysis grade) was shaken several times with concentrated H_2SO_4 , washed with water and with a 5% aqueous solution of NaHCO_3 , dried over MgSO_4 , distilled from P_2O_5 , and subsequently distilled from sodium.²⁶ Methylene chloride was purified by the method

described in ref 26 including refluxing with H_2SO_4 , washing, and distillation from CaH_2 .

Kinetic Studies. The stock solution of the catalyst in toluene was prepared by dissolving under nitrogen gas a known quantity of $\text{B}(\text{C}_6\text{F}_5)_3$ in carefully prepurified toluene. The reaction was carried out in a glass 10 mL reactor equipped with magnetic stirrer and a three-way glass stopcock connected to a nitrogen gas circulating system. The reactor was immersed in a thermostated silicone oil bath. The reactor was thoroughly purged with nitrogen, and known amounts of substrates and gas chromatographic standard were introduced by means of tight precision Hamilton syringe while nitrogen gas was allowed to flow through the stopcock. By the same technique the zero sample was withdrawn, and a known amount of the solution of $\text{B}(\text{C}_6\text{F}_5)_3$ in toluene was introduced. Usually the time of the introduction of catalyst was considered as the zero time of reaction; however, in some cases, when an induction period was observed, the zero time was found by extrapolation. Samples were withdrawn by Hamilton syringe and introduced to Eppendorfer vessels containing 4-ethylpyridine used for quenching of the reaction. The samples were subjected to gas chromatographic analysis.

Simultaneous Kinetic and Spectroscopic Studies. The reaction was carried out in a glass reactor to which a quartz cell of 0.1 cm path length was fused. The reactor was placed in the thermostated compartment of the UV spectrometer. The method of performing the reaction as well as the sampling and analytical procedures were described above. During the course of the reaction the spectrum of the reaction mixture was registered at timed intervals during the course of the reaction.

Analytical Methods. The gas chromatographic analyses were performed using a Hewlett-Packard HP 6890 chromatograph equipped with thermal conductivity detector and HP1 capillary column of 30 m length and 0.53 mm diameter. The carrier gas was helium, flow rate 5 mL/min. The injector and detector temperatures were both 250 °C. The column temperature was programmed: 3 min 40 °C isoth, 60–240 °C at 10 °C/min, 10–20 min 240 °C isoth. Conditions of taking chromatograms were selected to obtain a good separation of peaks. *n*-Dodecane was used as internal standard. The response factors were mostly determined from the analysis of isolated compound. Assignment of peaks was based on the results of GC-MS analysis.

Mass spectra were recorded on a GC-MS Finnigan MAT 95 instrument using chemical ionization technique. The reactive gas (H^+ carrier) was isobutane at a pressure of 10^{-4} Torr. The mass spectrometer was working in tandem with a gas chromatograph through which selected samples of the quenched reaction mixture were directed to the ionization chamber of the mass spectrometer.

UV spectra were recorded on a Hewlett-Packard UV-vis 8453 spectrometer. Quartz cells having path lengths of 0.1, 0.5, and 1 cm were used. The cells were placed in a thermostated compartment of the spectrometer. They were fused

(26) Perrin, D. D.; Armarego, W. L. F.; Perrin, D. R. *Purification of Laboratory Chemicals*; Pergamon Press: Oxford, 1966.

through a pass to a glass three-way stopcock, which was connected to a reservoir with nitrogen gas to ensure a positive pressure of N_2 in the cell.

The fluorescence spectrum was recorded on a Perkin-Elmer Luminescence Spectrometer LS50.

Computational Methods. Geometries of all model species were optimized with B3LYP/6-31G* using the Gaussian 03 package,²⁷ with the hybrid density functional B3LYP/6-31G* method.²⁸ Stationary points were confirmed by vibrational analysis. Final single-point electronic energies were obtained at the B3LYP/6-311+G(2d,p) level of theory. This level of calculation is conventionally denoted as B3LYP/6-311+G(2d,p)/B3LYP/6-31G*. Vibrational components of the thermal energy were scaled by 0.98. Enthalpies of complex formation were calculated at 298 K using corrections obtained from frequency analysis, including rotational and translational terms. Energies and enthalpies of complex formation were corrected for the basis set superposition error (BSSE)²⁹ using the counterpoise option built in the Gaussian program. At this level of theory, these corrections were in the range 0.2–0.5 kcal/mol. Partial atomic charges, Wiberg bond orders, and orbital analysis were performed using the NBO theory.³⁰ Vertical excitation energies (only for singlet excited states) were calculated using the time-dependent DFT model (TD-B3LYP/6-31+G*³¹). All calculations were performed for the gas-phase conditions.

Acknowledgment. The financial support from General Electric Company is gratefully acknowledged.

Supporting Information Available: Cartesian coordinates of the B3LYP/6-31G*-optimized structures of the $\text{H}_2\text{O}-\text{B}(\text{C}_6\text{F}_5)_3$, $\text{Me}_3\text{SiH}-\text{B}(\text{C}_6\text{F}_5)_3$, and $(\text{H}_3\text{Si})_3\text{O}-\text{HB}(\text{C}_6\text{F}_5)_3$ complexes. This material is available free of charge via the Internet at <http://pubs.acs.org>.

OM050563P

(27) Frisch, M. J.; Trucks, G. W.; Schlegel, H. B.; Scuseria, G. E.; Robb, M. A.; Cheeseman, J. R.; Montgomery, J. A., Jr.; Vreven, T.; Kudin, K. N.; Burant, J. C.; Millam, J. M.; Iyengar, S. S.; Tomasi, J.; Barone, V.; Mennucci, B.; Cossi, M.; Scalmani, G.; Rega, N.; Petersson, G. A.; Nakatsuji, H.; Hada, M.; Ehara, M.; Toyota, K.; Fukuda, R.; Hasegawa, J.; Ishida, M.; Nakajima, T.; Honda, Y.; Kitao, O.; Nakai, H.; Klene, M.; Li, X.; Knox, J. E.; Hratchian, H. P.; Cross, J. B.; Bakken, V.; Adamo, C.; Jaramillo, J.; Gomperts, R.; Stratmann, R. E.; Yazyev, O.; Austin, A. J.; Cammi, R.; Pomelli, C.; Ochterski, J. W.; Ayala, P. Y.; Morokuma, K.; Voth, G. A.; Salvador, P.; Dannenberg, J. J.; Zakrzewski, V. G.; Dapprich, S.; Daniels, A. D.; Strain, M. C.; Farkas, O.; Malick, D. K.; Rabuck, A. D.; Raghavachari, K.; Foresman, J. B.; Ortiz, J. V.; Cui, Q.; Baboul, A. G.; Clifford, S.; Cioslowski, J.; Stefanov, B. B.; Liu, G.; Liashenko, A.; Piskorz, P.; Komaromi, I.; Martin, R. L.; Fox, D. J.; Keith, T.; Al-Laham, M. A.; Peng, C. Y.; Nanayakkara, A.; Challacombe, M.; Gill, P. M. W.; Johnson, B.; Chen, W.; Wong, M. W.; Gonzalez, C.; and Pople, J. A. *Gaussian 03*, Revision C.02; Gaussian, Inc.: Wallingford, CT, 2004.

(28) Becke, A. D. *J. Chem. Phys.* **1993**, *98*, 5648.

(29) Boys, S. F.; Bernardi, F. *Mol. Phys.* **1970**, *19*, 553.

(30) Reed, A. E.; Curtiss, L. A.; Weinhold, F. *Chem. Rev.* **1988**, *88*, 899. Glendening, E. D.; Reed, A. E.; Carpenter, J. E., Weinhold, F. *NBO Version 3.1*.

(31) Bauernschmitt, R.; Ahlrichs, R. *Chem. Phys. Lett.* **1996**, *256*, 454.